Pergamon

Scripta Materialia, Vol. 41, No. 5, pp. 461–465, 1999
Elsevier Science Ltd

1359-6462/99/$–see front matter

PII S1359-6462(99)00191-8

TENSION/COMPRESSION ASYMMETRY IN CREEP BEHAVIOR OF A Ni-BASED SUPERALLOY

K. Kakehi
Department of Mechanical Engineering, Tokyo Metropolitan University, 1-1 Minami-Osawa, Hachioji, Tokyo 192-0397, Japan

(Received May 21, 1999)
(Accepted June 1, 1999)

Keywords: Ni-based superalloy; Single crystal; Creep strength; Tension/compression; Asymmetry

Introduction

Orientation and temperature dependence of yield stress or CRSS (Critical Resolved Shear Stress) and tension/compression anisotropy of the yield stress or CRSS have been shown by Shah and Duhl (1), Heredia and Pope (2), and Miner *et al.* (3). Tension/compression asymmetry in the yield strength of Ni-based superalloys has been explained in terms of the "core width effect" (4). Shah and Duhl (5) observed the tension/compression asymmetry in creep deformation, which is similar to that observed in the yield strength, and indicated that it can be attributed to cross slip and dislocation core-constriction mechanisms associated with octahedral slip. However, little is known about the mechanism of tension/compression asymmetry in creep.

In the present study, single crystals of a Ni-base superalloy were subjected to tensile and compressive creep tests. Tension/compression asymmetry in creep behavior was examined in detail for each orientation.

Experimental Procedure

The investigation was carried out on an experimental Ni-based superalloy. Its chemical composition is listed in Table 1. Single crystals of this alloy were grown from a melt by the modified Bridgman method. After the analysis of the crystallographic orientation by the back-reflection Laue method, the tensile and compressive specimens for creep tests were cut from the as-grown crystals by a spark cutter. The specimens were solutionized at 1255°C for 10 h aged at 1100°C for 10 h. They were then cooled in an air blast. Creep tests were performed at 700°C under a nominal stress of 820 MPa for three major orientations, [001], [011] and [$\bar{1}$11]. The cube edge length and volume fraction of the γ' precipitates were measured by scanning electron microscopy.

TABLE 1
Chemical Composition of the Superalloy (mass %)

Cr	Mo	Co	W	Ta	Ti	Al	V	Ni
10.11	2.50	9.97	0.04	0.07	4.75	5.73	0.93	Bal.

Results and Discussion

The mean edge length of primary cuboidal γ' precipitates was 0.40 μm and the volume fraction was 60% following the aging treatment. As shown in Figure 1, superfine secondary precipitates were observed in the matrix channel. Figure 2 shows the tensile and compressive creep curves for each orientation. In the Ni-based superalloy tested in this study, {111}<112>-type slip systems were found to be operative during creep at 700°C (6); therefore, the shear strain for {111}<112>-type slip systems was plotted along the vertical axis. In the [001] orientation (Fig. 2(a)), the compressive creep curve showed inferior strength compared to the tensile creep curve; whereas, the creep behavior for tensile/compressive stresses is completely reversed in the [011] orientation (Fig. 2(b)). The [011]-tensile specimen showed extremely poor creep strength and large rupture elongation. The rupture life was less than 10 h in contrast to over 500 h for the [001]-tensile specimen. The inferior strength in [011]-tensile creep is attributed to the formation of a mechanical twin that extends over both γ-γ' phases (6). The tensile creep mechanism was found to be different between the orientations favored for the $(\bar{1}11)[1\bar{1}2]$ slip system and those favored for the $(111)[\bar{2}11]$ slip system (6). The [001] orientation is favored for the $(\bar{1}11)[1\bar{1}2]$ slip system, while the [011] orientation is favored for the $(111)[\bar{2}11]$ slip system. In tensile creep deformation, the $(\bar{1}11)[1\bar{1}2]$ slip system is generated by partial dislocation shearing of γ-γ' phases during primary creep. TEM observation showed the formation of intrinsic/extrinsic stacking fault pairs, which necessitates reactions between perfect dislocations of the matrix with unlike a/2<110> Burgers vectors (7–9). TEM studies also revealed that a a/3<112> partial dislocation can be created simply by the dissociation of a perfect a/2<110> dislocation at the γ-γ' interface (10,11). Irrespective of the prominent mechanism for dislocation dissociation in the γ' precipitates, it is obvious that the $(\bar{1}11)[1\bar{1}2]$ planar slip is due to partial dislocation shearing of both γ-γ' phases during the primary creep, and that small mean surface-to-surface spacing between precipitates promotes the activity of the $(\bar{1}11)[1\bar{1}2]$ slip system (6,12). On the other hand, the $(111)[\bar{2}11]$ slip in tensile creep is generated by a mechanical twin (6,9).

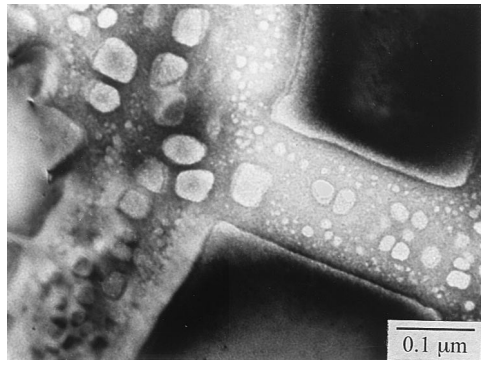

Figure 1. Superfine secondary γ' precipitates were observed in the matrix channel after aging for 10 h at 1100°C.

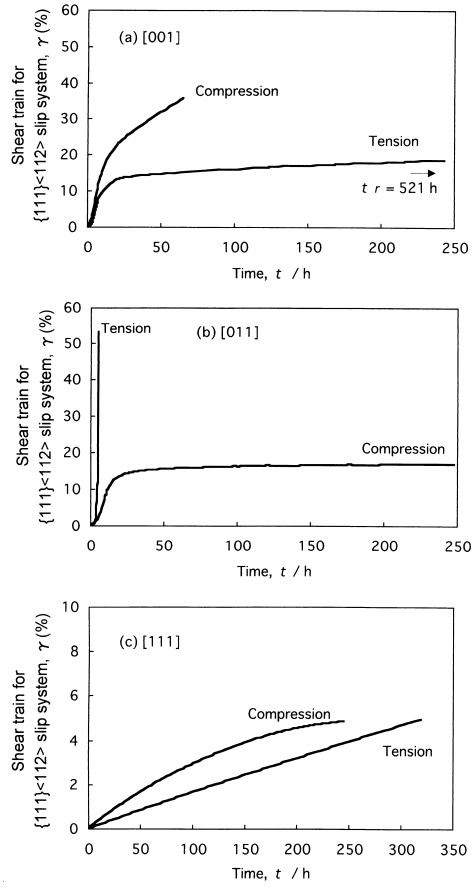

Figure 2. Tensile and compressive creep curves in (a) [001], (b) [011] and (c) [$\bar{1}11$] orientations at 700°C/820 MPa. Tension/compression asymmetry was observed in [001] and [011] orientations.

In compressive creep, as shown in Figure 3, the TEM micrograph of the [001] specimen showed the microtwin lamellae that extend over both γ-γ' phases (Figure 3 (a)); whereas the microtwin lamellae could not be observed in the [011]-compressive specimen (Figure 3 (b)). Twinning is not a dominant deformation mechanism in metals which possess many possible slip systems, and it generally occurs when the slip systems are restricted or when something increases the critical resolved shear stress so that the twinning stress is less than the stress for slip (13). The yield stress of γ' precipitates increases with increasing temperature up to a peak temperature (650°C ~ 800°C). Since the critical stress for twinning will be lower than that for the slip near the peak temperature, novel mechanical twins would occur in the Ni-based superalloy. The twinning shear is always directional in the sense that the shear in one direction is not equivalent to the shear in the opposite direction. Twinning in FCC metals occurs on {111} planes in the <112> direction. The atomic movements by twinning are illustrated in Figure 4 (14). **E** is the atomic position after the occurrence of twinning deformation. The shaded atom **A** can move easily in the [$\bar{1}1\bar{2}$] direction but the atom **J** is hindered from moving in the [$1\bar{1}2$] direction by the top face of atom **B**; therefore, twinning occurs by the shear on the ($\bar{1}11$) plane in the [$\bar{1}1\bar{2}$] direction but not by the shear in the opposite direction. In [011]-tensile and [001]-compressive creep deformations, the resolved shear stress on the {111} plane acts in the twinning direction, and the formation of

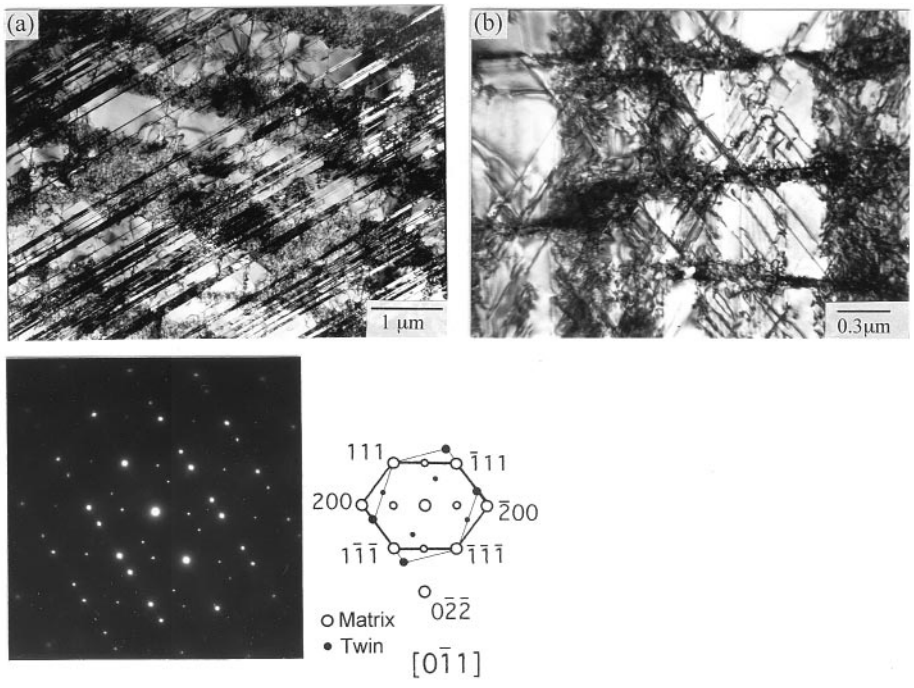

Figure 3. TEM micrographs of compressive creep specimens in (a) [001] and (b) [011] orientations. The foils were cut along the {011} planes. Electron diffraction pattern of central area of (a), which indicates that thin plates are mechanical twins.

mechanical twin results in weak creep strength. As shown in Figure 2 (a) and (b), the [001]-tensile creep curve was in agreement with the [011]-compressive creep curve. In [001]-tensile and [011]-compressive creep deformations, the resolved shear stress acts in the anti-twinning direction. Since it is impossible to form twins, γ' precipitates would be sheared by the pair of superlattice intrinsic/extrinsic stacking faults.

In $[\bar{1}11]$ specimens, compared with [001] and [011] specimens, both tensile and compressive resolved shear strains were less than 6% (axial strain, $\varepsilon = 1.9\%$) at 250 h. Both in the tensile and compressive creep deformations, creep strain is mainly created by the dislocation motions in the matrix channel (15–17); therefore, asymmetry of creep curves was not observed. In the single-aged specimen used in this study, the hyperfine secondary precipitates were observed (Figure 1) and remained undissolved during the creep test (6). They prevented the dislocation motions in the matrix channel and resulted in an extremely low creep rate and strain (Figure 2(c)).

Conclusion

Tension/compression asymmetry of creep strength in [001] and [011] orientations is attributed to the directional-formation characteristic of a mechanical twin. In $[\bar{1}11]$ specimens, creep strain is created by dislocation motions in the matrix channel; therefore, tension/compression asymmetry of creep curves was not observed.

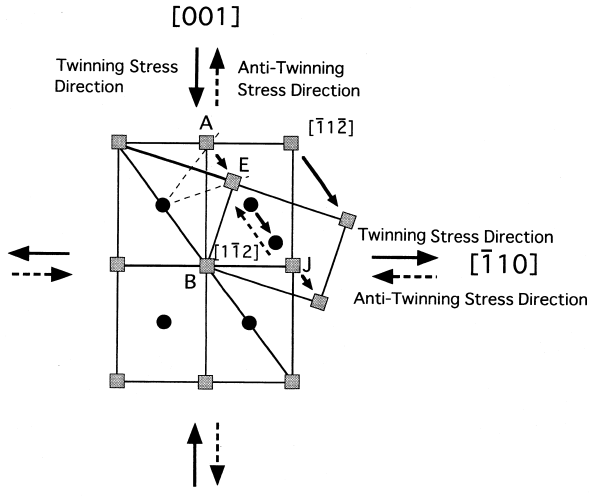

Figure 4. Plan view of the (110) plane in a FCC crystal lattice showing the upper right half of the lattice twinned on the ($\bar{1}11$) [$\bar{1}1\bar{2}$] system. The atoms in the (110) plane layer are shown as squares, while atoms under the atomic layer are indicated by circles.

References

1. D. M. Shah and D. N. Duhl, Superalloys 1984, p. 105, The Metallurgical Society of AIME, Warrendale, PA (1984).
2. F. E. Heredia and D. P. Pope, Acta Metall. 34, 279 (1986).
3. R. V. Miner, T. P. Gabb, J. Gayda, and K. J. Hemker, Metall. Trans. A. 17A, 507 (1986).
4. C. Lall, S. Chin, and D. P. Pope, Metall. Trans. A. 10A, 1323 (1979).
5. D. M. Shah and D. N. Duhl, Superalloys 1988, p. 693, The Metallurgical Society of AIME, Warrendale, PA (1988).
6. K. Kakehi, Metall. Mater. Trans. A. 30A, 1249 (1999).
7. B. H. Kear, G. R. Leverant, and J. M. Oblak, Trans. ASM. 62, 639 (1969).
8. B. H. Kear, J. M. Oblack, and A. F. Giamei, Metall. Trans. 1, 2477 (1970).
9. B. H. Kear, Order-Disorder Transformations in Alloys, ed. by H. Warlimont, p. 440, Springer-Verlag, New York (1974).
10. M. Condat and B. Décamp, Scripta Metall. 21, 607 (1987).
11. P. Caron, T. Khan, and P. Veyssiére, Phil. Mag. A. 57, 859 (1988).
12. P. R. Bhowal, E. F. Wright, and E. L. Raymond, Metall. Trans. A. 21A, 1709 (1990).
13. G. E. Dieter, Mechanical Metallurgy, 3rd edn., p. 132, McGraw-Hill Book Co., New York (1986).
14. W. F. Hosford, The Mechanics of Crystals and Textured Polycrystals, p. 169, Oxford University Press, New York (1993).
15. V. Sass, U. Glatzel, and M. Feller-Kniepmeier, Acta Metall. Mater. 44, 1967 (1996).
16. R. Völkl, U. Glatzel, and M. Feller-Kniepmeier, Scripta Metall. Mater. 31, 1481 (1994).
17. D. Bettge and W. Österle, Scripta Mater. 40, 389 (1999).